Electrochemical Analysis of Bicapped Triangular Cobalt Cyclopentadienyl Clusters, $[Co_3(\eta^5\text{-}C_5H_{5-x}Me_x)_3(\mu_3\text{-}X)(\mu_3\text{-}Y)]^n$ (x = 0, 1, 5), Containing Mixed π-Acceptor X and π-Donor Y Capping Ligands (X = CO, NO; Y = $NSiMe_3$, $NC(O)NH_2$, NH): Pronounced Variations in Redox Behavior as a Function of Coordinating Ligands

Robert L. Bedard and Lawrence F. Dahl*

Contribution from the Department of Chemistry, University of Wisconsin—Madison, Madison, Wisconsin 53706. *Received September 12, 1985*

Abstract: The recent preparation of a series of 48-electron $Co_3(\eta^5\text{-}C_5H_{5-x}Me_x)_3(\mu_3\text{-}X)(\mu_3\text{-}Y)$ clusters (x = 0, 1, 5) containing π-acceptor X ligands (X = CO, NO) and π-donor (nonhybridized) Y ligands (Y = NR, NH) provided the impetus for a systematic cyclic voltammetric investigation. This exploratory work involving an assessment of the electrochemical effects of variations in the nature of the terminal and capping ligands was stimulated by a previous lack of redox data on nitrene (NH)- or organonitrene (RN)-capped clusters and on triangular metal clusters containing mixed π-acceptor and π-donor capping ligands. The redox behavior of these new metal clusters was found to be intriguingly varied and highly unusual. Each of the three carbonyl–organonitrene and two carbonyl–nitrene capped neutral clusters containing cyclopentadienyl or methylcyclopentadienyl ligands exhibited one two-electron oxidation to a 46-electron species and one two-electron reduction to a 50-electron species. All of these two-electron couples are reversible except for those of the $Co_3(\eta^5\text{-}C_5H_4Me)_3(\mu_3\text{-}CO)(\mu_3\text{-}NH)$ cluster (IIb) which are viewed as being quasireversible. In sharp constrast, the OC, HN-bicapped $Co_3(\eta^5\text{-}C_5Me_5)_3(\mu_3\text{-}CO)(\mu_3\text{-}NH)$ cluster (IIc) displayed two successive reversible one-electron oxidations to 47- and 46-electron species and a reversible one-electron reduction to a 49-reduction species. Each of the 48-electron ON, HN-bicapped $[Co_3(\eta^5\text{-}C_5H_{5-x}Me_x)_3(\mu_3\text{-}NO)(\mu_3\text{-}NH)]^+$ monocations (x = 0, IIIa; x = 1, IIIb) was found to undergo two reversible one-electron reductions to the neutral cluster and the monoanion. The resulting stereochemical-bonding implications of the simultaneous two-electron transfer behavior in the C_5H_5- and C_5H_4Me-containing neutral clusters vs. the one-electron transfer behavior in the corresponding C_5Me_5-containing cluster (IIc) were examined. A comparative analysis of the $E_{1/2}$ values of the Me_3SiN-capped clusters (Ia, Ib) and the HN-capped clusters (IIa, IIb) was found to be consistent with the greater π-acceptor influence of the $NSiMe_3$ capping ligand; likewise, the small differences found between the corresponding $E_{1/2}$ values in the three C_5H_5-containing clusters (Ia, IIa, IIIa) and their C_5H_4Me-containing derivatives (Ib, IIb, IIIb) were observed to reflect the enhanced electron-donating ability of the C_5H_4Me ligand. Visible absorption spectra were obtained for the two OC, Me_3SiN-bicapped clusters (x = 0, Ia; x = 1, Ib) and three OC, HN-bicapped clusters (x = 0, IIa; x = 1, IIb; x = 5, IIc); the difference between the spectral band patterns of the Me_3SiN-capped and HN-capped clusters was rationalized in terms of electronic considerations. Electrochemical evidence is given that the $[Co_3(\eta^5\text{-}C_5H_5)_3(\mu_3\text{-}CO)(\mu_3\text{-}NH)]^{2+}$ dication, which is generated by a two-electron oxidation of $Co_3(\eta^5\text{-}C_5H_5)_3(\mu_3\text{-}CO)(\mu_3\text{-}NH)$ (IIa), undergoes deprotonation with triethylamine to form the $[Co_3(\eta^5\text{-}C_5H_5)_3(\mu_3\text{-}CO)(\mu_3\text{-}N)]^+$ monocation with a "bare" pyramidal-like nitrido-capped ligand. A reexamination of the oxidation behavior of the classical Fischer–Palm 49-electron $Ni_3(\eta^5\text{-}C_5H_5)_3(\mu_3\text{-}CO)_2$ cluster is also presented. Contrary to prior electrochemical and chemical evidence, this cyclic voltammetric investigation revealed that both the Fischer–Palm cluster and its C_5H_4Me-containing derivative undergo reversible one-electron oxidations to give 48-electron monocations.

In an extensive series of papers, Robinson,[1-6] Simpson,[1-6] Bond,[1,2,6] Vahrenkamp,[6,7] and their co-workers have described systematic electrochemical and spectroscopic (IR, ESR, electronic) investigations of a large number of monocapped triangular metal carbonyl clusters. Representative compounds studied included not only the 48-electron $Co_3(CO)_9(\mu_3\text{-}ER)$ clusters (E = C, Ge, R = Me, Ph) and their Lewis base derivatives (e.g., $Co_3(CO)_{9-x}L_x(\mu_3\text{-}CR)$ (x = 1–3; L = R_3P, $(RO)_3P$, RCN; R = Me, Ph) but also heteronuclear metal species with $Co_2M(\mu_3\text{-}ER)$ cores (M = Cr, Mo, W, E = C, Ge, R = Me, Ph; M = Fe, E = P, R = Me, Ph) and $CoMM'(\mu_3\text{-}PR)$ cores (M = Fe, M' = Mo, Ni, R = Me, Ph). The 48-electron homonuclear cobalt clusters were generally found to undergo an electrochemically and chemically reversible one-electron reduction to the respective 49-electron monoanions. Several Lewis base derivatives (for x = 3) also exhibited an electrochemically reversible one-electron oxidation at low temperature and/or fast scan rates, but reversible oxidizability was not determined to be a general characteristic of any of these monocapped trimetal carbonyl systems. Although several of the above heteronuclear metal clusters (formally derived from a tricobalt nonacarbonyl cluster by substitution of electronically equivalent fragments) such as $FeCo_2(CO)_9(\mu_3\text{-}S)$ similarly exhibited one-electron reductions, the electrochemical behavior of most mixed metal systems was complex (depending on the capping group and number of disparate metal atoms) which made the cyclic voltammetric data difficult to interpret.

In contrast to the above comprehensive electrochemical investigations of a large variety of triangular metal carbonyl clusters, electrochemical studies of the redox behavior of triangular metal cyclopentadienyl clusters have been comparatively limited to date.

In 1966 Dessy et al.[8] showed from combined polarographic and voltammetric measurements that the classical Fischer–Palm

(1) Bond, A. M.; Peake, B. M.; Robinson, B. H.; Simpson, J.; Watson, D. J. *Inorg. Chem.* **1977**, *16*, 410–415.
(2) Bond, A. M.; Dawson, P. A.; Peake, B. M.; Rieger, P. H.; Robinson, B. H.; Simpson, J. *Inorg. Chem.* **1979**, *18*, 1413–1417.
(3) Peake, B. M.; Robinson, B. H.; Simpson, J.; Watson, D. J. *Inorg. Chem.* **1977**, *16*, 405–409.
(4) (a) Peake, B. M.; Rieger, P. H.; Robinson, B. H.; Simpson, J. *Inorg. Chem.* **1979**, *18*, 1000–1005. (b) Peake, B. M.; Rieger, P. H.; Robinson, B. H.; Simpson, J. *Inorg. Chem.* **1981**, *20*, 2540–2543.
(5) (a) Colbran, S.; Robinson, B. H.; Simpson, J. *J. Chem. Soc., Chem. Commun.* **1982**, 1361–1362. (b) Colbran, S. B.; Robinson, B. H.; Simpson, J. *Organometallics* **1983**, *2*, 943–951. (c) Colbran, S. B.; Robinson, B. H.; Simpson, J. *Organometallics* **1983**, *2*, 952–957.
(6) Lindsay, P. N.; Peake, B. M.; Robinson, B. H.; Simpson, J.; Honrath, U.; Vahrenkamp, H.; Bond, A. M. *Organometallics* **1984**, *3*, 413–426.
(7) (a) Honrath, U.; Vahrenkamp, H. *Z. Naturforsch.* **1984**, *39b*, 545–554. (b) Honrath, U.; Vahrenkamp, H. *Z. Naturforsch.* **1984**, *39b*, 555–558.
(8) Dessy, R. E.; King, R. B.; Waldrop, M. *J. Am. Chem. Soc.* **1966**, *88*, 5112-5121.

0002-7863/86/1508-5933$01.50/0

$Ni_3(\eta^5\text{-}C_5H_5)_3(\mu_3\text{-}CO)_2$ molecule would undergo a reversible one-electron reduction, but did not present any evidence for possible oxidation. A later proposal (based upon an experimental–theoretical analysis of a related monocapped tricobalt cluster) by Strouse and Dahl[9] that the unpaired electron in this 49-electron bicapped trimetal cluster should occupy a trimetal antibonding MO gave rise to unsuccessful attempts in our laboratories to oxidize and isolate the corresponding 48-electron monocation of $Ni_3(\eta^5\text{-}C_5H_5)_3(\mu_3\text{-}CO)_2$ for a structural-bonding analysis. A formal removal of the unpaired electron in this cluster was subsequently achieved with the preparation and structural characterization of the closely related 48-electron cobalt–dinickel $(\eta^5\text{-}C_5H_{5-x}Me_x)CoNi_2(\eta^5\text{-}C_5H_5)_2(\mu_3\text{-}CO)_2$ series ($x = 0, 1, 5$).[10a] Comparative electrochemical measurements showed that each of these diamagnetic compounds undergoes a reversible one-electron reduction to a 49-electron system. The observation of a negative linear change in the $E_{1/2}$ values for the reduction couple as a function of sequential substitution of x methyl substituents in place of hydrogens was rationalized from electronic energetic arguments involving the antibonding trimetal LUMO to which the unpaired electron is added. This work in turn led to the preparation and structural-bonding analysis of the 50-electron Fischer–Palm monoanion, the 49-electron $[(\eta^5\text{-}C_5Me_5)CoNi_2(\eta^5\text{-}C_5H_5)_2(\mu_3\text{-}CO)_2]^-$ monoanion, and the 49-electron $Ni_3(\eta^5\text{-}C_5Me_5)_3(\mu_3\text{-}CO)_2$.[10b] Cyclic voltammetric measurements of the latter pentamethylcyclopentadienyl analogue of the Fischer–Palm molecule indicated a reversible reduction to the 50-electron monoanion and two reversible one-electron oxidations to the 48- and 47-electron systems. The conspicuous absence of any electrochemical or chemical evidence for oxidation of the Fischer–Palm (unsubstituted) cyclopentadienyl trinickel cluster to a cationic species was noted again and rationalized in terms of bonding considerations.[10b]

A systematic electrochemical investigation was reported by Madach and Vahrenkamp[11] in 1981 for seven bicapped trimetal clusters, viz., $Ni_3(\eta^5\text{-}C_5H_5)_3(\mu_3\text{-}CO)_2$, $M_3(\eta^5\text{-}C_5H_5)_3(\mu_3\text{-}S)_2$ (where M = Co, Ni), $Co_3(\eta^5\text{-}C_5H_5)_3(\mu_3\text{-}S)(\mu_3\text{-}CS)$, and $Fe_3(CO)_9(\mu_3\text{-}X)(\mu_3\text{-}Y)$ (where X = CO, Y = S; X = Y = S; X = S, Y = SO). Their electrochemical data indicated that $Ni_3(\eta^5\text{-}C_5H_5)_3(\mu_3\text{-}CO)_2$ undergoes a reversible one-electron reduction but only irreversible oxidations; their data pointed to reversible one-electron processes for $Co_3(\eta^5\text{-}C_5H_5)_3(\mu_3\text{-}S)_2$ (one reduction and two oxidations), $Ni_3(\eta^5\text{-}C_5H_5)_3(\mu_3\text{-}S)_2$ (one reduction and one oxidation), $Co_3(\eta^5\text{-}C_5H_5)_3(\mu_3\text{-}S)(\mu_3\text{-}CS)$ (one reduction), and $Fe_3(CO)_9(\mu_3\text{-}S)_2$ (one reduction).

More recently, cyclic voltammetric studies of a series of 48-electron bis(μ_3-carbyne)tricobalt cyclopentadienyl clusters, $Co_3(\eta^5\text{-}C_5H_5)_3(\mu_3\text{-}CR)(\mu_3\text{-}CR')$ (R = R' = Ph, Fc; R = H, R' = Ph, $SiMe_3$, Fc; R = Me_3Si, R' = I where Fc denotes ferrocenyl), were reported by Colbran, Robinson, and Simpson.[12a] These clusters generally were found to undergo an electrochemically and chemically reversible one-electron oxidation. At approximately the same time, Kawamura and co-workers[12b] reported the electrochemical oxidation and chemical reduction of $Co_3(\eta^5\text{-}C_5H_5)_3(\mu_3\text{-}CPh)_2$ to give the 47-electron monocation and 49-electron monoanion; ESR studies of both radicals provided a foundation for their proposed electronic structures of this bicapped trimetal $[Co_3(\eta^5\text{-}C_5H_5)_3(\mu_3\text{-}CPh)_2]^n$ series ($n = 1+, 0, 1-$).

The recent preparation (preceding paper[13a]) of a series of 48-electron $Co_3(\eta^5\text{-}C_5H_{5-x}Me_x)_3(\mu_3\text{-}XO)(\mu_3\text{-}NR)$ clusters (X = C, N) containing one π-acidic OC- or ON-capped ligand and one π-donor (nitrene) HN- or (organonitrene) RN-capped ligand

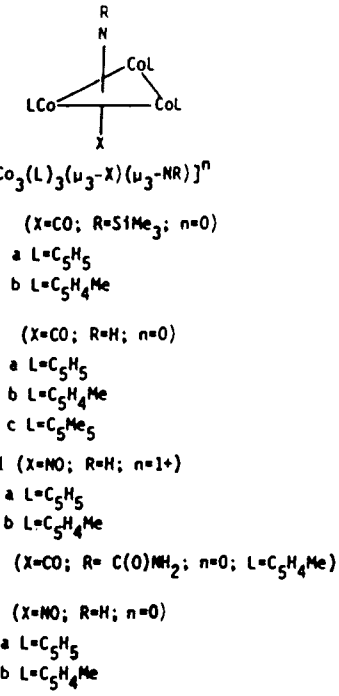

Figure 1. Abbreviation scheme for the 48-electron mixed-ligand bicapped tricobalt clusters.

(Figure 1) was the impetus for the systematic electrochemical investigation presented here. The fact that no previous redox studies had been reported on RN-capped clusters or for that matter on bicapped trimetal clusters with mixed (π-donor)–(π-acceptor) capping ligands made this cyclic voltammetric study of particular relevance to our efforts to explore the effects due to variations in the nature of the ligands on the physicochemical properties of these clusters. The redox behavior of these new clusters is intriguingly varied when compared to that of other triangular metal clusters. Several of these mixed-ligand capped clusters exhibit two-electron oxidation and reduction processes (uncommon for metal clusters), while others display successive one-electron oxidations and reductions. The observed marked changes in electrochemical reponse are shown to be directly related to the nature of the terminal C_5R_5 rings as well as of the capping ligands.

A new examination of the redox properties of the Fischer–Palm $Ni_3(\eta^5\text{-}C_5H_5)_3(\mu_3\text{-}CO)_2$ molecule and of the corresponding methylcyclopentadienyl analogue, $Ni_3(\eta^5\text{-}C_5H_4Me)_3(\mu_3\text{-}CO)_2$, is also presented. Contrary to prior electrochemical and chemical evidence,[8,10,11] this cyclic voltammetric study shows that both the Fischer–Palm molecule and C_5H_4Me analogue exhibit reversible oxidation behavior in the time scale of the CV measurement to give 48-electron monocations.

Another major project stemming from these electrochemical studies has involved the isolation of oxidized and/or reduced species for X-ray crystallographic determination in order to correlate the redox-generated variations in geometry with changes in electronic configuration. This goal has been achieved with respect to one of these mixed ligand bicapped trimetal systems; those results will be given in the following paper.[13b]

Experimental Section

Materials. The tricobalt clusters, $Co_3(\eta^5\text{-}C_5H_{5-x}Me_x)_3(\mu_3\text{-}CO)(\mu_3\text{-}NSiMe_3)$ ($x = 0$, Ia; $x = 1$, Ib), $Co_3(\eta^5\text{-}C_5H_{5-x}Me_x)_3(\mu_3\text{-}CO)(\mu_3\text{-}NH)$ ($x = 0$, IIa; $x = 1$, IIb; $x = 5$, IIc), the $[Co_3(\eta^5\text{-}C_5H_{5-x})_3(\mu_3\text{-}NO)(\mu_3\text{-}NH)]^+$ monocations ($x = 0$, IIIa; X = 1, IIIb), and $Co_3(\eta^5\text{-}C_5H_4Me)_3(\mu_3\text{-}CO)(\mu_3\text{-}NC(O)NH_2)$ (IV) (Figure 1) were prepared as described elsewhere.[13a] The Fischer–Palm $Ni_3(\eta^5\text{-}C_5H_5)_3(\mu_3\text{-}CO)_2$ was prepared by a literature method.[14] The methylcyclopentadienyl analogue, $Ni_3(\eta^5\text{-}C_5H_4Me)_3(\mu_3\text{-}CO)_2$, was synthesized by CS_2 reflux of $Ni_2(\eta^5\text{-}C_5H_4Me)_2(\mu_2\text{-}CO)_2$.[15] Its IR spectrum in hexane displayed a triply

(9) (a) Strouse, C. E.; Dahl, L. F. *Discuss. Faraday Soc.* **1969**, *47*, 93–106. (b) Strouse, C. E.; Dahl, L. F. *J. Am. Chem. Soc.* **1971**, *93*, 6032–6041.

(10) (a) Byers, L. R.; Uchtman, V. A.; Dahl, L. F. *J. Am. Chem. Soc.* **1981**, *103*, 1942–1951. (b) Maj, J. J.; Rae, A. D.; Dahl, L. F. *J. Am. Chem. Soc.* **1982**, *104*, 3054–3063.

(11) Madach, T.; Vahrenkamp, H. *Chem. Ber.* **1981**, *114*, 505–512.

(12) (a) Colbran, S. B.; Robinson, B. H.; Simpson, J. *Organometallics* **1984**, *3*, 1344–1353. (b) Enoki, S.; Kawamura, T.; Yonezawa, T. *Inorg. Chem.* **1983**, *22*, 3821–3824.

(13) (a) Bedard, R. L.; Rae, A. D.; Dahl, L. F. *J. Am. Chem. Soc.*, preceding paper in this issue. (b) Bedard, R. L.; Dahl, L. F. *J. Am. Chem. Soc.*, following paper in this issue.

(14) Fischer, E. O.; Palm, C. *Chem. Ber.* **1958**, *91*, 1725–1731.

bridging carbonyl frequency at 1747 cm^{-1}; an X-ray structural determination substantiated its identity.[15]

All solvents (viz., THF, CH_2Cl_2, and CH_3CN) utilized for electrochemical measurements were initially dried over standard agents. Further purification of each solvent involved three (freeze–pump)–thaw cycles on a high-vacuum line followed by treatment with activated 3A molecular sieves (Linde) for 12 h, after which the solvent was vacuum-transferred and stored in rigorously dried glass vessels with greaseless high-vacuum stopcocks. The supporting electrolyte, tetrabutylammonium hexafluorophosphate ($TBAPF_6$), was recrystallized three times from absolute ethanol and dried for 2 days in a drying pistol under vacuum at boiling toluene temperature.

Electrochemical Measurements. Cyclic voltammetric data were obtained with a BAS-100 Electrochemical Analyzer which features *iR*-compensation circuitry.[16] All cyclic voltammetry was undertaken with the electrochemical cell enclosed in a N_2-filled Vacuum Atmospheres drybox. The working electrode used was a platinum disk, and the reference electrode was a porous Vycor-tipped aqueous SCE separated from the test solution by a Vycor-tipped salt bridge with a 0.1 M $TBAPF_6$/CH_3CN filling solution. The tip of the salt bridge was situated approximately 5 mm from the working electrode. The counter electrode was a platinum coil, and the solution volumes were ca. 5 mL with a concentration of ca. 10^{-3} M of cluster compound. Electrochemical data are summarized in Table I for cyclic voltammograms recorded at a scan rate of 100 mV/s. As also found for other clusters, the $E_{1/2}$ values for the reduction couples reported here are solvent-dependent, although relative voltages within a given voltammogram are consistent in different solvent systems. Points of zero faradaic current flow (i.e., null points) were determined by linear sweep voltammetry under vigorous stirring. The null points were taken as those current plateaus in the voltammograms with essentially zero-measured current.

Spectral Measurements. UV–visible spectra were recorded on a Cary 17D spectrometer with a 1.0 mm path length and quartz cells equipped with high-vacuum stopcocks. Solutions of 10^{-3}–10^{-4} M compound in THF were used. All infrared spectra were obtained on a Beckman IR 4240 spectrophotometer.

Determination of the Number of Electrons (*n*) Involved in the Electrode Reaction. (a) General. Evidence for the number of electrons (*n*) in a given redox couple was obtained by three different methods.

(b) Estimation of *n* from Infrared Spectral Analysis. (1) Oxidation of Ib in a Single Two-Electron Step (*n* = 2). In a typical experiment, Ib (65.0 mg; 0.123 mmol) and $Ag(SO_3CF_3)$ oxidant (31.6 mg; 0.123 mmol) were stirred in 20 mL of CH_2Cl_2 for 2 h, during which time the solution changed color from brown-green to red-brown. After removal of the solvent under vacuum, an infrared spectrum (KBr pellet) of the solid residue revealed a substantial amount of starting cluster (Ib), as evidenced by a carbonyl band at 1670 cm^{-1} and another higher frequency band at 1760 cm^{-1} which was assigned as the carbonyl stretching frequency of the oxidized cluster. The comparable intensities of these two bands indicated an approximate 50% conversion of Ib to an oxidized species.

This mixture was redissolved in CH_2Cl_2, and another equivalent of $Ag(SO_3CF_3)$ (30.0 mg; 0.117 mmol) was added. After the mixture was stirred for another hour, the solvent was removed. Another infrared spectrum (KBr pellet) of the resulting solid residue showed only the above new carbonyl band at 1760 cm^{-1}. The absence of the characteristic carbonyl band for Ib signifying that the parent cluster was completely converted to the oxidized species provides prime evidence that Ib undergoes a single two-electron oxidation to a relatively stable dication. The dication derived by reacting 2 equiv of oxidant to Ia possessed a similar IR spectrum (KBr pellet) with a carbonyl frequency at 1767 cm^{-1}.

Repeated experiments with either $Ag(SO_3CF_3)$ or $[Fe(C_5H_5)_2]^+$-$[SO_3CF_3]^-$ as oxidants gave similar results which expectedly were invariant to reaction times of 1–8 h. After the addition of 1 equiv of oxidizing agent, approximately one-half of the starting clusters Ia or Ib could be extracted out of the residue with toluene. Complete conversion to a stable dication (more stable in the case of Ib) occurred within 1 h upon treatment with 2 equiv of oxidant. The solid oxidized product from Ib could be stored under N_2 in a freezer for several days. Considerable effort to crystallize the dication of Ib was expended. Dichloromethane, THF, and acetone solutions of the oxidized species were slowly diffused into nonpolar solvents such as cyclohexane and benzene, but the cluster appeared to disproportionate (after a time span of 10–12 h) into an insoluble residue and a solution of Ib (as analyzed by IR and ^1H NMR spectra).

(2) Oxidation of IIc in a Single One-Electron Step (*n* = 1). In a typical experiment, IIc (15.0 mg; 24 μmol) and $[Fe(C_5H_5)_2]^+[SO_3CF_3]^-$ (8.0 mg; 24 μmol) were weighed into a flask in a Vacuum Atmospheres drybox. Dry CH_2Cl_2 was added, and the solution was stirred for 2 h. The solvent was then pumped off under vacuum, and the ferrocene was removed by repeated washing with toluene. An infrared spectrum (KBr pellet) of the solid residue established from the absence of the characteristic carbonyl band for IIc at 1665 cm^{-1} that all starting material (IIc) had reacted. The appearance of a new strong carbonyl band at a higher frequency of 1720 cm^{-1} is thereby attributed to the oxidized species being a monocation (corresponding to $n = 1$). Infrared spectra indicated that the monocation of IIc was stable as a solid for several days when stored under N_2 in a freezer.

(c) Estimation of *n* by Peak–Current Comparison. In the first experiment, equimolar quantities of IIa (2.5 mg; 6.0 μmol) and neutral $Co_3(\eta^5\text{-}C_5H_5)_3(\mu_3\text{-}NO)(\mu_3\text{-}NH)$ (Va) (2.5 mg; 6.0 μmol) were dissolved in 5 mL of 0.1 M $TBAPF_6$/THF solution. The peak currents determined from a cyclic voltammogram of this solution were 57 μA for IIa and 27 μA for Va. The resulting peak–current ratio of 2.11/1 corresponds to a single two-electron oxidation process ($n = 2$) for IIa based upon a known value of $n = 1$ for the oxidation of Va to IIIa (vide infra). Since an estimated error of ±0.2 mg in weighing on the Cahn electronic analytical balance located inside the Vacuum Atmospheres drybox gives rise to an estimated uncertainty of ca. 8% in an individual peak current, the observed peak–current ratio is within the estimated experimental error of 16% for this experiment.

In a second analogous experiment, approximately equimolar quantities of IIc (3.0 mg; 4.8 μmol) and neutral $Co_3(\eta^5\text{-}C_5H_4Me)_3(\mu_3\text{-}NO)(\mu_3\text{-}NH)$ (Vb) (2.6 mg; 5.2 μmol) were dissolved in 5 mL of 0.1 M $TBAPF_6$/CH_2Cl_2 solution. A cyclic voltammogram of this solution gave peak currents of 17 μA for IIc and 21 μA for Vb, corresponding to a peak–current ratio of 0.81/1. The estimated error in weighing the samples and thus in the peak current per couple was 7%. Since the molar ratio (based on the weighed quantities) for the two compounds was 0.92/1, the determined peak–current ratio is within an estimated error of 14%. Since the oxidation of Vb to IIIb has an *n* value of one (vide infra), this experiment established that the reduction couples for IIc were likewise one-electron processes.

In a third analogous experiment, a measurement of peak currents for equimolar quantities of Ia and Va also gave a peak–current ratio of ca. 2/1, thereby substantiating the assignment of both redox couples for Ia as two-electron processes.

(d) Determination of *n* by Isolation of the Reduced Species Vb from IIIb. In this reaction, equimolar quantities of IIIb and cobaltocene were stirred at room temperature in a THF solution which immediately turned to a deep red-brown color. After 1 h a large amount of a yellow-brown solid (presumably containing the cobaltocenium ion) precipitated. Removal of solvent followed by extraction with three 10-mL portions of toluene gave a dark red-brown solution of the desired neutral product Vb which was unambiguously characterized by X-ray crystallographic and spectroscopic analyses as described elsewhere.[13b] A cyclic voltammogram of Vb was identical with that of IIIb except that the most positive redox couple correponded in VB to a one-electron oxidation process and in IIIb to a one-electron reduction process.

Similar treatment of IIIa with cobaltocene also gave rise to a quantitative conversion to a neutral toluene-soluble product which was identified as Va from spectroscopic measurements. A cyclic voltammetric examination of Va similarly showed that this compound and the monocation IIIa were related by one-electron redox processes.

Cyclic Voltammetric Deprotonation Study of the Electrochemically Generated Dication of IIa. In a typical experiment, a 10^{-3} M solution of IIa in 0.1 M $TBAPF_6/CH_2Cl_2$ was placed in the electrochemical cell, and the single two-electron oxidation couple corresponding to the $IIa \rightleftarrows IIa^{2+} + 2e^-$ process was examined by cyclic voltammetry. Successive portions of triethylamine were added via syringe. A rescanning of the above redox couple after each addition of Et_3N showed a continuous decrease in the cathodic current but no noticeable change in the anodic current. No further addition of Et_3N was made after the cathodic current was reduced to zero. At this point an excess of $HBF_4 \cdot Et_2O$ was added. A reexamination of the redox couple showed a complete regeneration of the cathodic wave with the i_c/i_a ratio again being unity.

Results and Discussion

Electrode Processes for the Cyclopentadienyl Clusters Ia and IIa and for the Methylcyclopentadienyl Clusters Ib, IIb, and IV. (a) General. These 48-electron cyclopentadienyl and methylcyclopentadienyl cobalt clusters have similar redox properties as determined from a comparison of their cyclic voltammograms and tabulated electrochemical data (Table I). Each cluster exhibits

(15) Englert, M. H. Ph.D. Thesis, University of Wisconsin—Madison, 1983.

(16) He, P.; Avery, J. P.; Faulkner, L. R. *Anal. Chem.* **1982**, *54*, 1313A–1326A.

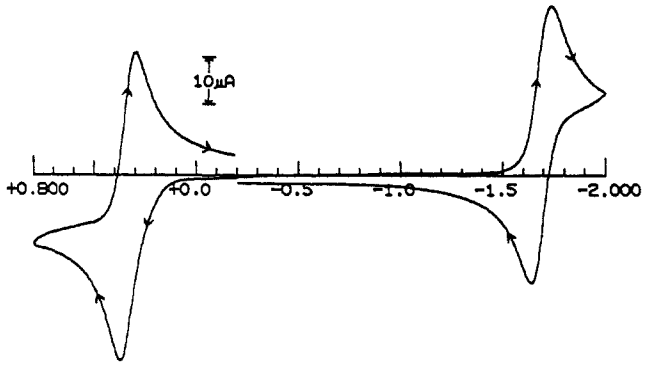

Figure 2. Cyclic voltammogram for the oxidation and reduction of $Co_3(\eta^5\text{-}C_5H_4Me)_3(\mu_3\text{-}CO)(\mu_3\text{-}NSiMe_3)$ (Ib) in THF/0.1 M $TBAPF_6$ at a platinum disk electrode with a scan rate of 100 mV/s. A reversible two-electron oxidation occurs at $E_{1/2} = +0.33$ V, and a reversible two-electron reduction occurs at $E_{1/2} = -1.68$ V (vs. SCE). The couples are shown as separately scanned to emphasize reversibility.

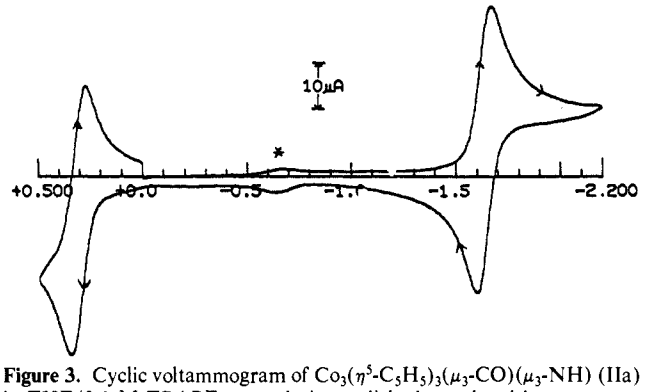

Figure 3. Cyclic voltammogram of $Co_3(\eta^5\text{-}C_5H_5)_3(\mu_3\text{-}CO)(\mu_3\text{-}NH)$ (IIa) in THF/0.1 M $TBAPF_6$ at a platinum disk electrode with a scan rate of 100 mV/s. A reversible two-electron oxidation occurs at $E_{1/2} = +0.31$ V, and a reversible two-electron reduction occurs at $E_{1/2} = -1.63$ V (vs. SCE). The presumed effect of a small electroactive impurity is indicated by an asterisk.

a reduction and an oxidation couple. All couples (except those for IIb) are reversible, as evidenced by the fact that for each couple the peak-current ratio (i_a/i_c) is unity and the separation (ΔE_p) between the potentials corresponding to the cathodic and anodic peak currents is nearly independent of scan rate between 50 and 500 mV/s. That both couples for IIb are quasireversible is revealed from Table I which shows that the peak-current ratio for each couple deviates by 20% from unity and that the associated ΔE_p values, which possess a marked scan-rate dependence, are substantially larger than those for the reversible couples for the other four clusters. Furthermore, the quasireversible nature of each couple in IIb was found to be somewhat electrode-dependent. When a freshly cleaned, glassy carbon working electrode (PAR) was utilized in place of the platinum one, substantially improved reversible characteristics in both redox couples of IIb were observed at slower scan rates.

Figures 2, 3, and 4 show representative cyclic voltammograms for Ib, IIa, and IV, respectively. The similarity of the relative peak heights for both couples within a given voltammogram points to the same number of electrons (n) being involved in the oxidation and reduction of each of these clusters. Not shown in these figures is that for each cluster an irreversible oxidation process occurs between +1.0 and +1.1 V. Sweeping through this irreversible process for each of the clusters invariably led to extensive contamination of the electrode surface which necessitated a repolishing of the platinum working electrode.

A combination of infrared spectral analyses and peak-current comparisons[6] of cyclic voltammograms for equimolar mixtures of two clusters was used to determine the number of electrons involved in the oxidation and reduction steps for each of the five 48-electron $Co_3(\eta^5\text{-}C_5H_{5-x}Me_x)_3(\mu_3\text{-}CO)(\mu_3\text{-}NR)$ clusters (for R = $SiMe_3$, Ia ($x = 0$) and Ib ($x = 1$); for R = H, IIa ($x = 0$) and

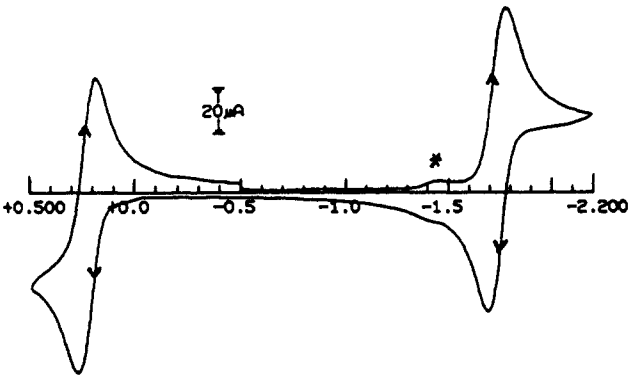

Figure 4. Cyclic voltammogram of $Co_3(\eta^5\text{-}C_5H_4Me)_3(\mu_3\text{-}CO)(\mu_3\text{-}NC(O)NH_2)$ (IV) in THF/0.1 M $TBAPF_6$ at a platinum disk electrode with a scan rate of 100 mV/s. A reversible two-electron oxidation occurs at $E_{1/2} = +0.22$ V, and a reversible two-electron reduction occurs at $E_{1/2} = -1.63$ V (vs. SCE). The presumed effect of a small electroactive impurity is indicated by an asterisk.

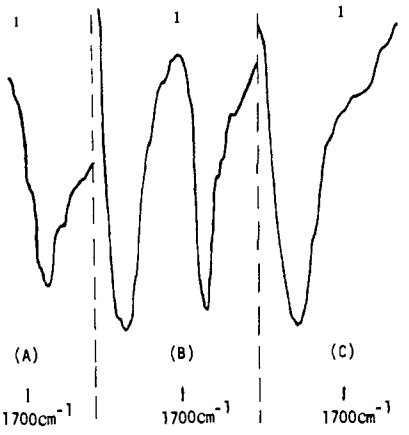

Figure 5. Solid-state (KBr pellet) infrared spectra in the triply bridging carbonyl region (1800–1600 cm^{-1}) upon oxidation of Ib with Ag^+ oxidant: (A) before addition of $Ag(SO_3CF_3)$ (spectrum of starting material Ib); (B) after reaction with 1 equiv of $Ag(SO_3CF_3)$ (spectrum of 50:50 mixture of Ib and $[Ib]^{2+}$ dication); and (C) after reaction with 2 equiv of $Ag(SO_3CF_3)$ (spectrum of $[Ib]^{2+}$ dication).

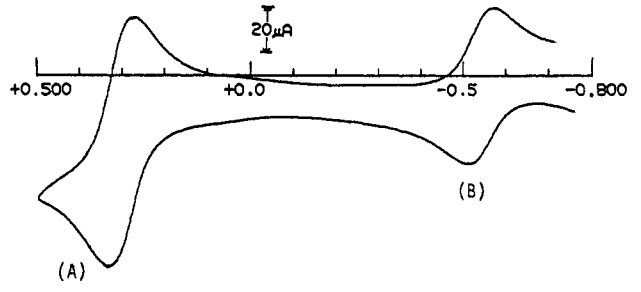

Figure 6. Cyclic voltammogram showing oxidations of equimolar concentrations of $Co_3(\eta^5\text{-}C_5H_5)_3(\mu_3\text{-}CO)(\mu_3\text{-}NH)$ (IIa) and a reference cluster $Co_3(\eta^5\text{-}C_5H_5)_3(\mu_3\text{-}NO)(\mu_3\text{-}NH)$ (Va), in THF/0.1 M $TBAPF_6$ at a platinum disk electrode with a scan rate of 100 mV/s. The relative peak currents in the voltammogram establish the reversible couple at (A) to correspond to a two-electron oxidation of IIa to the $[IIa]^{2+}$ dication based on the reversible couple at (B) corresponding to an independently determined one-electron oxidation of Va to its monocation (IIIa).

IIb ($x = 1$); for R = $NC(O)NH_2$, IV ($x = 1$)). Figure 5 presents solid-state spectra (KBr pellet) in the triply bridging carbonyl region for Ib as a function of 0, 1, and 2 equiv of added Ag^+ oxidant. An infrared spectrum (Figure 5B) of the solid mixture resulting from the reaction of Ib with 1 equiv of Ag^+ reveals two strong carbonyl bands—one corresponding to the spectrum of unreacted Ib (Figure 5A) and the other (at expectedly higher frequency) corresponding to a cationic species of Ib. After reaction of this presumed 50:50 mixture with a second equivalent of Ag^+,

Table I. Electrochemical Data on 48-Electron $[Co_3(\eta^5\text{-}C_5R_5)_3(\mu_3\text{-}X)(\mu_3\text{-}NR')]^n$ Species[a]

species	solvents	oxidations				reductions			
		$E_{1/2}$ (V)	ΔE_p (mV)	i_a/i_c	n'	$E_{1/2}$ (V)	ΔE_p (mV)	i_a/i_c	n'
I (X = CO; R'= $SiMe_3$; n = 0)									
(a) C_5H_5	THF	+0.40	80	1.0	2	−1.60	95	1.0	2
(b) C_5H_4Me	THF	+0.33	90	1.0	2	−1.68	90	1.0	2
II (X = CO; R' = H; n = 0)									
(a) C_5H_5	THF	+0.31	69	1.0	2	−1.63	71	1.0	2
(b) C_5H_4Me	THF	+0.25	160	0.8	2	−1.76	120	1.2	2
(c) C_5Me_5	THF	−0.07	65	1.0	1	−2.03	60	1.0	1
	CH_2Cl_2	−0.21	100	1.0	1				
		+0.75	80	1.0	1				
III (X = NO; R' = H; n = 1+)									
(a) C_5H_5	CH_3CN					−0.53	64	1.0	1
						−1.49	91	1.0	1
(b) C_5H_4Me	CH_3CN					−0.60	77	1.0	1
						−1.58	97	1.0	1
IV (X = CO; R' = $NC(O)NH_2$; n = 0; C_5H_4Me)	THF	+0.22	90	1.0	2	−1.73	90	1.0	2

[a] $E_{1/2}$ denotes the mean potential between the peak potentials E_p; ΔE_p is the difference between the two peak potentials; i_a/i_c denotes the peak current ratio; and n' is the determined number of electrons for a given couple. Data are for a scan rate of 100 mV/s.

an IR spectrum (Figure 5C) shows complete conversion of Ib to the new oxidized species. These spectral data clearly establish that the oxidation of Ib is a two-electron process. That IIa also undergoes a two-electron oxidation process was demonstrated from an electrochemical experiment involving the use of Va which was independently shown (vide supra) to undergo a reversible one-electron oxidation to IIIa. A cyclic voltammogram (Figure 6) of equimolar concentrations of IIa and Va displayed a 2.1:1 peak–current ratio for the oxidation process of IIa relative to that of Va. The analogous occurrence of a two-electron oxidation process for Ib was also shown from another electrochemical experiment in which a cyclic voltammogram of equimolar concentrations of Ib and Vb similarly exhibited a 2.0:1 current–peak ratio for the oxidation couple of Ib relative to that of Vb. A ratio of range 2.0–2.8:1 is expected based upon the assumptions of equivalent diffusion coefficients and equivalent concentrations for both electroactive species undergoing *reversible* processes; the 2.8:1 ratio corresponds to the second electron transfer being easier than the first electron transfer in the reversible two-electron process. A cyclic voltammogram of an equimolar mixture of IV and Vb (from which n = 1) gave a peak–current ratio of 1.8:1 for their oxidation couples. This observed variation from the expected range is possibly due to the presence of a nonelectroactive impurity in the sample of IV, which resulted in a smaller quantity of IV in solution than that calculated from the weighed quantities.

In light of the close similarities in ligation and structure of the five 48-electron bicapped tricobalt clusters containing one π-acidic OC-capped ligand and one π-donor RN-capped ligand, it is not at all surprising that their redox characteristics are similar. However, to our knowledge there are no previous reports of reversible two-electron transfer processes for any triangular metal cyclopentadienyl or carbonyl clusters.

(b) Implications of Simultaneous Two-Electron Transfer Behavior. The observed two-electron process in the reversible or quasireversible interconversion of each neutral cluster to its dication (or dianion) is presumed to be a consequence of the cluster giving up (or accepting) a second electron with nearly the same or even greater facility than giving up (or accepting) the first electron.[17-22] Since both the HOMO and LUMO in these 48-electron clusters possess considerable trimetal antibonding character, either the removal of one or two electrons from the HOMO or the addition of one or two electrons to the LUMO would bring about marked geometrical changes affecting the entire $Co_3(CO)(NR)$ core. Although the $E_{1/2}$ value is a measure of the energy difference between the reduced and oxidized species (including solvent effects and other variables), it is presumed from qualitative considerations that the $E_{1/2}$ value for these closely related clusters correlates with the energy of the HOMO for the reduced species with a more stable HOMO requiring greater energy for electron removal. Therefore, we rationalize that the single two-electron reduction of the neutral 48-electron parent to its 50-electron dianion is a consequence of the much greater HOMO stabilization in the 50-electron system relative to that in the 49-electron system due to a large structural change which more than compensates for greater electrostatic repulsions due to the second electron. Similarly, a greater HOMO stabilization in the 46-electron system relative to that in the 47-electron system due to different geometrical configurations may be invoked to account for the single two-electron oxidation of the 48-electron cluster to its 46-electron dication. Collman et al.[23] have utilized a similar energetic argument in rationalizing the observed single two-electron step in the reduction of the (metal–metal)-bonding $Fe_2(CO)_6(\mu_2\text{-}PPh_2)_2$[24] to give its (metal–metal)-nonbonding dianion[25] with a resultant dramatic change in geometry.

(17) Richardson and Taube[18] developed a simple model[19] for estimating the conproportionation constant, K_c, for a two-step charge transfer from the observed peak-to-peak voltage separation, ΔE_p, of a single two-electron couple in a cyclic voltammogram. Although the Richardson–Taube model has been applied[20] to obtain the K_c for an electrochemical two-electron reduction of a gold cluster, we did not utilize this method to determine K_c for the bicapped tricobalt clusters because the experimental ΔE_p values obtained from cyclic voltammograms of a number of organometallic clusters are considerably larger than theoretical values for both oxidation and reduction couples which are judged to be reversible by other criteria (e.g., i_a/i_c = 1; $E_{1/2}$ independent of scan rate; i_p proportional to $v^{1/2}$).[5b,c,6,21,22]

(18) Richardson, D. E.; Taube, H. *Inorg. Chem.* **1981**, *20*, 1278–1285.

(19) The Richardson–Taube model[18] involves the determination of $E^\circ = E^\circ(1) - E^\circ(2)$ for a two-step electrochemical charge transfer of the type

$$A \xrightarrow{E^\circ(1)} B \xrightarrow{E^\circ(2)} C$$

where $E^\circ(1)$ and $E^\circ(2)$ are the standard potentials for two one-electron steps. The concentrations of the species A, B, and C at equilibrium are given by the conproportionation constant, K_c, where

$$K_c = [B]^2/[A][C] = \exp[\Delta E^\circ/25.69) \text{ at } 298 \text{ K}$$

For cyclic voltammetric measurements, E° (in mV) is approximated as $E_{1/2}$ which can be obtained from $E_{1/2}$ values tabulated by Richardson and Taube[18] as a function of the observed peak-to-peak voltage separation, ΔE_p, for a two-electron couple.

(20) Van der Linden, J. G. M.; Paulissen, M. L. H.; Schmitz, J. E. J. *J. Am. Chem. Soc.* **1983**, *105*, 1903–1907.

(21) The effects of slow two-electron transfers and disproportionation on cyclic voltammograms have been analyzed by Ryan.[22]

(22) Ryan, M. D. *J. Electrochem. Soc.* **1978**, *125*, 547-555.

(23) Collman, J. P.; Rothrock, R. K.; Finke, R. G.; Moore, E. J.; Rose-Munch, F. *Inorg. Chem.* **1982**, *21*, 146–156.

(24) Huntsman, J. R. Ph.D. Thesis, University of Wisconsin—Madison, 1973.

(25) Ginsburg, R. E.; Rothrock, R. K.; Finke, R. G.; Collman, J. P.; Dahl, L. F. *J. Am. Chem. Soc.* **1979**, *101*, 6550–6562.

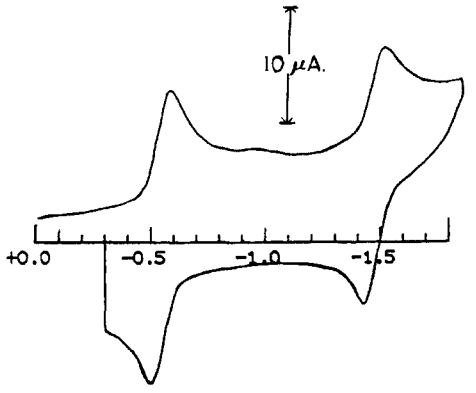

Figure 7. Cyclic voltammogram of the 48-electron $[Co_3(\eta^5\text{-}C_5H_5)_3(\mu_3\text{-}NO)(\mu_3\text{-}NH)]^+$ monocation (IIIa) in CH_3CN/0.1 M $TBAPF_6$ at a platinum disk electrode with a scan rate of 100 mV/s. Two reversible one-electron reductions occur at $E_{1/2} = -0.53$ V and $E_{1/2} = -1.49$ V (vs. SCE). The first reduction produces the neutral 49-electron cluster Va.

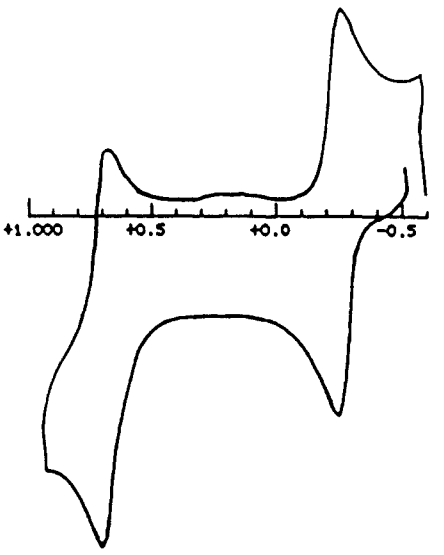

Figure 8. Cyclic voltammogram of $Co_3(\eta^5\text{-}C_5Me_5)_3(\mu_3\text{-}CO)(\mu_3\text{-}NH)$ (IIc) in CH_2Cl_2/0.1 M $TBAPF_6$ at a platinum disk electrode with a scan rate of 100 mV/s. Two reversible one-electron oxidations occur at $E_{1/2} = -0.21$ V and $E_{1/2} = +0.75$ V (vs. SCE).

Another striking example of a compound which exhibits a reversible two-electron charge transfer is tetramethyltetracyanoquinodimethane (TMTCNQ) whose synthesis and properties were recently reported by Cowan and co-workers.[26] In sharp contrast to TCNQ, MeTCNQ, 2,5-Me_2TCNQ, and bis(ethano)TCNQ[27] (a bis(cyclobutane-fused)tetracyanoquinodimethane), all of which exhibit two one-electron reductions with similar potentials, a cyclic voltammogram of TMTCNQ revealed only one two-electron reduction. On the basis of a comparison with bis(ethano)TCNQ, Cowan and co-workers[26] concluded that the novel redox characteristics of TMTCNQ, which is presumed to be nonplanar due to overcrowding of the four methyl substituents, are the result of steric rather than electronic effects.

(c) Comparative Analysis of the $E_{1/2}$ Values of Me_3Si-Capped Clusters (Ia, Ib) and the HN-Capped Clusters (IIa, IIb): The π-Acceptor Influence of the (μ_3-NSiMe$_3$) Ligand. Table I shows that one salient feature of the electrochemical behavior of these $Co_3(\eta^5\text{-}C_5H_{5-x}Me_x)_3(\mu_3\text{-}CO)(\mu_3\text{-}NR)$ clusters ($x = 0, 1$) is that a Me_3SiN-capped cluster is both harder to oxidize and easier to reduce than a corresponding HN-capped cluster. The greater difficulty in oxidizing a Me_3SiN-capped cluster in THF is shown from the corresponding $E_{1/2}$ values for the 2+/0 couples being 80–90 mV more positive for a Me_3SiN-capped cluster than for the respective HN-capped cluster, viz., +0.40 V for Ia vs. 0.31 V for IIa; +0.33 V for Ib vs. +0.25 V for IIb. Likewise, the 2−/0 reduction couples of the Me_3SiN-capped clusters in THF are less negative than those for the corresponding HN-capped clusters, viz., −1.60 V for Ia vs. −1.63 V for IIa; −1.68 V for Ib vs. −1.76 V for IIb. These data are consistent with the premise that the μ_3-NSiMe$_3$ ligand is effectively functioning as a weaker σ electron donor and stronger π-acceptor than is a μ_3-NH ligand.

The sensitivity of the potentials to small variations in the electronic character of ligand substituents was also noted by Colbran, Robinson, and Simpson[12a] for the one-electron oxidations of two 48-electron $Co_3(\eta^5\text{-}C_5H_5)_3(\mu_3\text{-}CH)(\mu_3\text{-}CR)$ clusters (with $E_{1/2} = +0.53$ V for R = Ph; $E_{1/2} = +0.60$ V for R = $SiMe_3$). The difference in these $E_{1/2}$ values, which indicate that the PhC-capped cluster is easier to oxidize than the Me_3SiC-capped cluster, is also consistent with the μ_3-CSiMe$_3$ ligand being a weaker electron donor and stronger π-acceptor than is a μ_3-CPh ligand.

Similar electronic arguments have been utilized to account for the different $E_{1/2}$ values found in electrochemical reductions of organosilicon compounds where the difference in $E_{1/2}$ values for two compounds differing only by the substituent of a trimethylsilyl moiety for a methyl group has been attributed to a π-stabilization of the reduced species by the $SiMe_3$ group.[28] The π-acceptor behavior of a $SiMe_3$ substituent has also been well-documented in a number of spectroscopic, chemical, and theoretical studies.[29,30]

Electrode Processes for the $[Co_3(\eta^5\text{-}C_5H_{5-x}Me_x)_3(\mu_3\text{-}NO)(\mu_3\text{-}NH)]^+$ Monocations ($x = 0$, IIIa; $x = 1$, IIIb). The electrochemical propertes of IIIa and IIIb are similar; a representative cyclic voltammogram for IIIa is shown in Figure 7. Two reversible one-electron reduction couples of the parent monocation of the 49-electron neutral cluster and the 50-electron monoanion are observed. The similarity of the relative peak currents for both redox couples provides convincing evidence that each reduction involves the same number of electrons. That the first electrode process involves a one-electron transfer was ascertained from chemical reactions of both IIIa and IIIb with 1 equiv of cobaltocene reductant in THF to give quantitative yields of the 49-electron toluene-soluble neutral species Va and Vb. Details of the synthesis, characterization (including a crystal structure determination of Vb), and reactivities of these two clusters are given in the following paper.[13b]

Effects of the Terminal C_5H_5 vs. C_5H_4Me Ligands on the Redox Potentials in Ia vs. Ib, in IIa vs. IIb, and in IIIa vs. IIIb. The small differences found between the corresponding $E_{1/2}$ values (Table I) in the three C_5H_5-containing clusters (Ia, IIa, IIIa) and their C_5H_4Me-containing derivatives (Ib, IIb, IIIb) are as anticipated. The determined $E_{1/2}$ values, which for each couple are 60–130 mV less positive for the methylcyclopentadienyl derivative, show that the C_5H_4Me-containing cluster is easier to oxidize and more difficult to reduce than the correspoding C_5H_5-containing cluster (Ia, IIa, or IIIa). This normal trend (which prevails when unusual steric effects are absent) due to the enhanced electron-donating power of the C_5H_4Me ligand was previously observed and discussed[10a] from comparative cyclic voltammetric measurements on the 48-electron $(\eta^5\text{-}C_5H_{5-x}Me_x)CoNi_2(\eta^5\text{-}C_5H_5)_2(\mu_3\text{-}CO)_2$ series ($x = 0, 1, 5$).

(26) Kini, A.; Mays, M.; Cowan, D. *J. Chem. Soc., Chem. Commun.* **1985**, 286–287.
(27) Yamaguchi, S.; Tatemitsu, H.; Sakata, Y.; Enoki, T.; Misumi, S. *J. Chem. Soc., Chem. Commun.* **1982**, 1065–1066.
(28) (a) Alt, H.; Bock, H. *Tetrahedron* **1969**, *25*, 4825–4834. (b) Bock, H.; Alt, H. *Chem. Ber.* **1970**, *103*, 1784–1791.
(29) (a) Bock, H.; Alt, H. *J. Am. Chem. Soc.* **1969**, *92*, 1569–1576. (b) Jones, P. R.; Drews, M. J.; Johnson, J. K.; Wong, P. S. *J. Am. Chem. Soc.* **1972**, *94*, 4595–4599. (c) Symons, M. C. R. *J. Am. Chem. Soc.* **1972**, *94*, 8589–8590. (d) Griller, D.; Ingold, K. U. *J. Am. Chem. Soc.* **1973**, *95*, 6459–6460. (e) Ensslin, W.; Bock, H.; Becker, G. *J. Am. Chem. Soc.* **1974**, *96*, 2757–2762. (f) Jung, I. N.; Jones, P. R. *J. Am. Chem. Soc.* **1975**, *97*, 6102–6108.
(30) (a) Veszpremi, T.; Nagy, J. *J. Organomet. Chem.* **1983**, *255*, 41–47. (b) Sakurai, H.; Nakadaira, Y.; Hosomi, A.; Eriyama, Y.; Kabuto, C. *J. Am. Chem. Soc.* **1983**, *105*, 3359–3360. (c) Jellal, A.; Zahra, J.-P.; Santelli, M. *Tetrahedron Lett.* **1983**, *24*, 1395–1398. (d) Giordan, J. C. *J. Am. Chem. Soc.* **1983**, *105*, 6544–6546. (e) Paquette, L. A.; Uchida, T.; Gallucci, J. C. *J. Am. Chem. Soc.* **1984**, *106*, 335–340.

Table II. Redox Species of $[M_3(\eta^5\text{-}C_5R_5)_3(\mu_3\text{-}X)(\mu_3\text{-}Y)]^n$ Accessible by Cyclic Voltammetry

	species, no. of electrons				
series	46	47	48	49	50
$[Co_3(\eta^5\text{-}C_5H_{5-x}Me_x)_3(\mu_3\text{-}X)(\mu_3\text{-}NR')]^n$					
I (X = CO; R′ = $SiMe_3$; n = 0)					
(a) C_5H_5	n = 2+		n = 0		n = 2−
(b) C_5H_4Me	n = 2+		n = 0		n = 2−
II (X = CO; R′ = H; n = 0)					
(a) C_5H_5	n = 2+		n = 0		n = 2−
(b) C_5H_4Me	n = 2+		n = 0		n = 2−
(c) C_5Me_5	n = 2+	n = 1+	n = 0	n = 1−	
III (X = NO; R′ = H; n = 1+)					
(a) C_5H_5			n = 1+	n = 0	n = 1−
(b) C_5H_4Me			n = 1+	n = 0	n = 1−
$Ni_3(\eta^5\text{-}C_5H_{5-x}Me_x)(\mu_3\text{-}CO)_2$					
(a) C_5H_5 (n = 0)			n = 1+	n = 0	n = 1−
(b) C_5H_4Me (n = 0)			n = 1+	n = 0	n = 1−
(c) C_5Me_5 (n = 0)		n = 2+	n = 1+	n = 0	n = 1−

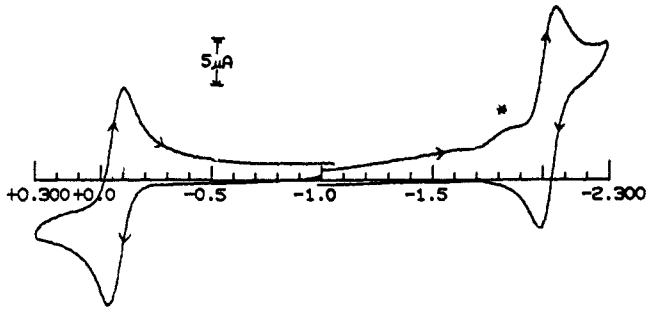

Figure 9. Cyclic voltammogram for the reduction and first oxidation couples (scanned separately to emphasize reversibility) of $Co_3(\eta^5\text{-}C_5Me_5)_3(\mu_3\text{-}CO)(\mu_3\text{-}NH)$ (IIc) in THF/0.1 M $TBAPF_6$ at a platinum disk electrode with a scan rate of 100 mV/s. A reversible one-electron oxidation occurs at $E_{1/2}$ = −0.07 V and a reversible one-electron reduction (not observed in the scan window of CH_2Cl_2) occurs at $E_{1/2}$ = −2.03 V (vs. SCE). The second one-electron oxidation which was observed at $E_{1/2}$ = +0.75 V in CH_2Cl_2 (Figure 8) is near the anodic limit (ca. +0.95 V vs. SCE) in THF, and hence solvent interactions interfere with the reversibility of this couple. The presumed effect of an electroactive impurity is indicated by an asterisk.

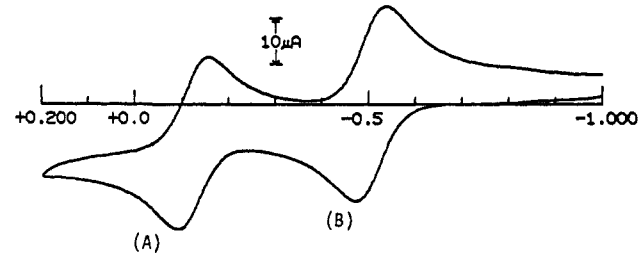

Figure 10. Cyclic voltammogram showing oxidations of equimolar concentrations of $Co_3(\eta^5\text{-}C_5Me_5)_3(\mu_3\text{-}CO)(\mu_3\text{-}NH)$ (IIc) and a reference cluster $Co_3(\eta^5\text{-}C_5H_4Me)_3(\mu_3\text{-}NO)(\mu_3\text{-}NH)$ (Vb), in CH_2Cl_2/0.1 M $TBAPF_6$ at a platinum disk electrode with a scan rate of 100 mV/s. The relative peak currents in the voltammogram established the reversible couple at (A) to correspond to a one-electron oxidation of IIc to the $[IIc]^+$ monocation based on the reversible couple at (B) corresponding to an independently determined one-electron oxidation of Vb to its monocation (IIIb).

Electrode Processes for $Co_3(\eta^5\text{-}C_5Me_5)_3(\mu_3\text{-}CO)(\mu_3\text{-}NH)$ (IIc). (a) General. This cluster shows a distinctly different redox behavior than its cyclopentadienyl (IIa) and methylcyclopentadienyl (IIb) analogues. A cyclic voltammogram (Figure 8) of IIc in CH_2Cl_2 exhibits two reversible oxidation processes at +0.75 and −0.21 V. Not shown is another irreversible oxidation within the solvent window at a more positive potential. A cyclic voltammogram (Figure 9) of IIc in THF shows a reversible oxidation couple at −0.07 V and a reversible reduction couple of comparable peak current at −2.03 V. A second oxidation couple observed in THF is at the anodic limit and hence was not reversible; this couple is reversible in CH_2Cl_2.

The similarity of the relative peak currents for the reversible couples of IIc in both CH_2Cl_2 and THF signifies that each reversible electron-transfer process involves the same number of electrons (n). That n = 1 was determined by two methods. In one experiment 1 equiv of the ferrocenium cation (as the $[SO_3CF_3]^-$ salt) was added to a dichlororomethane solution of IIc. An infrared spectrum of the isolated product, obtained after removal of ferrocene by several washings with hexane, did not display a triply bridging carbonyl band at 1665 cm^{-1} characteristic of the reactant IIc but instead exhibited a new strong carbonyl band at a higher frequency, 1720 cm^{-1}, thereby indicating a complete conversion of IIc to a stable oxidized product upon reaction with 1 equiv of a one-electron oxidizing agent. In a second experiment, a cyclic voltammogram (Figure 10) was obtained for an equimolar mixture of IIc and a standard Vb, which was independently shown to undergo a reversible one-electron oxidation to IIIb (vide supra). Similar relative peak currents found for both oxidations (A) and (B) gave further proof that the redox processes of IIc involve individual one-electron-transfer steps.

The above electrochemical analysis of IIc demonstrated that this neutral 48-electron cluster can be reversibly oxidized to the 47-electron monocation and 46-electron dication as well as reversibly reduced to the 49-electron monoanion (Table II).

(b) Electrochemical Differences Imposed by the Terminal Pentamethylcyclopentadienyl Ligands and Resulting Implications. The abrupt shift in electrochemical behavior of the bicapped-tricobalt $Co_3(CO)(NH)$ core from reversible two-electron charge-transfer processes for terminal C_5H_5 or C_5H_4Me ligands to reversible one-electron charge-transfer processes for terminal C_5Me_5 ligands is especially intriguing. The contrasting redox character of the C_5Me_5-containing IIc and the C_5H_5- and C_5H_4Me-containing IIa and IIb may be attributed to the combined influence of the markedly increased steric effects of the C_5Me_5 rings, which are tightly disposed about the central $Co_3(CO)(NH)$ core in IIc, and the considerably better electron-donating capacity of a C_5Me_5 ring. These factors are presumed to act in a cumulative fashion in destabilizing the filled HOMOs of both the neutral parent (IIc) and its dianion relative to the corresponding half-filled HOMOs of its monocation and monoanion, respectively. This greater energy destabilization of the filled HOMO of IIc relative to those of IIa and IIb and of the filled HOMO of the dianion of IIc relative to those of the dianions of IIa and IIb is due to smaller redox-generated geometrical distortions (on account of the markedly increased nonbonding interring interactions) for both IIc and its dianion and greater Co–C(ring) antibonding character in the HOMOs of both IIc and its dianion. Hence, the geometrically induced energy stabilization of each HOMO obtained from the added second electron is not large enough to overcome the increased electrostatic repulsion energy, such that both the 47-electron monocation and 49-electron monoanion are electrochemically accessible for IIc. The electrochemical reduction of the neutral 46-electron $Co_3(\eta^5\text{-}C_5Me_5)_3(\mu_3\text{-}CO)_2$, which likewise contains "sterically crowded" C_5Me_5 rings, is also a reversible one-electron charge-transfer process which results in the formation

Table III. Visible Spectral Data for Selected Clusters, $Co_3(\eta^5\text{-}C_5H_{5-x}Me_x)_3(\mu_3\text{-}CO)(\mu_3\text{-}NR)$ (x = 0, R = $SiMe_3$, Ia; x = 1, R = $SiMe_3$, Ib; x = 0, R = H, IIa; x = 1, R = H, IIb; x = 5, R = H, IIc)

species	λ_{max} (nm)	ϵ	λ_{max} (nm)	ϵ
Ia	443 sh	3000		
Ib	441 sh	4400		
IIa	416	4000	500 sh	1000
IIb	417	2500	500 sh	500
IIc	427	10000	531 sh	2500

of the 47-electron monoanion.[31] The redox-generated distortions of these bicapped metal clusters are discussed in more detail in the next paper.[13b]

Kadish and co-workers[32] recently showed from electrochemical studies that the oxo-bridged iron(III) tetraphenylporphyrin dimer, $[(TPP)Fe]_2(\mu_2\text{-}O)$, and the $[((p\text{-}Et_2N)TPP)Fe]_2(\mu_2\text{-}O)$ derivative, containing electron-donating diethylamino substituents on the four phenyl rings, may each be oxidized by four electrons. Of particular interest to us is that the greater electron-donating power of the (p-Et_2N)TPP ligand has a marked effect on the *relative* positions of the shifted redox couples, which consist of four separate one-electron reversible processes for the $[(PPP)Fe]_2(\mu_2\text{-}O)$ dimer and of two one-electron and one two-electron processes for the (p-Et_2N)TPP-substituted derivative. On the basis of the above electrochemical measurements showing nonlinear shifts in potentials upon substitution of strongly electron-donating substituents, we propose that a similar nonlinear substituent effect on the potentials may be dictating the electrochemical behavior of IIc such that the relative superimposed positions of the single steps in each two-electron redox process of IIa and IIb are completely resolved in IIc as two separate one-electron processes. An operational test for this hypothesis would be the preparation and electrochemical characterization of the $C_5H_3Me_2$-, $C_5H_2Me_3$-, and C_5HMe_4-containing analogues of IIc in order to determine whether each two-electron process in IIa or IIb shows a gradual splitting into two one-electron processes as a function of increased number of methyl substituents on the terminal $C_5H_{5-x}Me_x$ ligands. It is also tempting to speculate that part of the comparatively large ΔE_p separations for both redox couples of the C_5H_4Me-containing IIb (Table I) may be likewise ascribed to the above (methyl substituent)-induced ligand effect in increasing the $E_{1/2}$ value for the two one-electron steps in each two-electron process.

Electronic Absorption Spectra and Resulting Implications. Visible spectra for five 48-electron $Co_3(\eta^5\text{-}C_5H_{5-x}Me_x)_3(\mu_3\text{-}CO)(\mu_3\text{-}NR)$ clusters (R = $SiMe_3$, Ia (x = 0), Ib (x = 1); R = H, IIa (x = 0), IIb (x = 1), IIc (x = 5)) are shown in Figure 11, and spectral data are summarized in Table III. Each of the HN-capped clusters (IIa, IIb, IIc) exhibits a similar spectral pattern consisting of a broad band with a maximum at ca. 420 nm and a well-defined shoulder between 500 and 540 nm. In contrast, the R_3SiN-capped clusters (Ia and Ib) only have one characteristic shoulder at ca. 440 nm on a sharply rising band that extends into the UV region.

The nonparameterized Fenske–Hall MO model[33] has been utilized by Rives, You, and Fenske[34] to obtain the electronic structures of a series of bicapped-trimetal clusters including the 48-electron mixed-ligand $Co_3(\eta^5\text{-}C_5H_5)_3(\mu_3\text{-}CO)(\mu_3\text{-}S)$. Since this mixed triply bridged C_{3v} system with a π-acceptor OC-capped ligand and a π-donor S-capped ligand is a close relative of the above five $Co_3(CO)(NR)$ clusters, the MO correlation diagram calculated[34] for $Co_3(\eta^5\text{-}C_5H_5)_3(\mu_3\text{-}CO)(\mu_3\text{-}S)$ should be applicable to the RN-capped clusters. In this energy-level diagram, the filled HOMO is one of a closely spaced set of energy levels (labeled "t_{2g}"), while the nature of the LUMO is uncertain due to the unoccupied a_2 and e levels (labeled under C_{3v} symmetry) being very close in energy. Despite these complications, a comparative spectral analysis (given below) allows conclusions to be made regarding the qualitative influence of the RN-capped and C_5Me_5 ligands on the electronic structure.

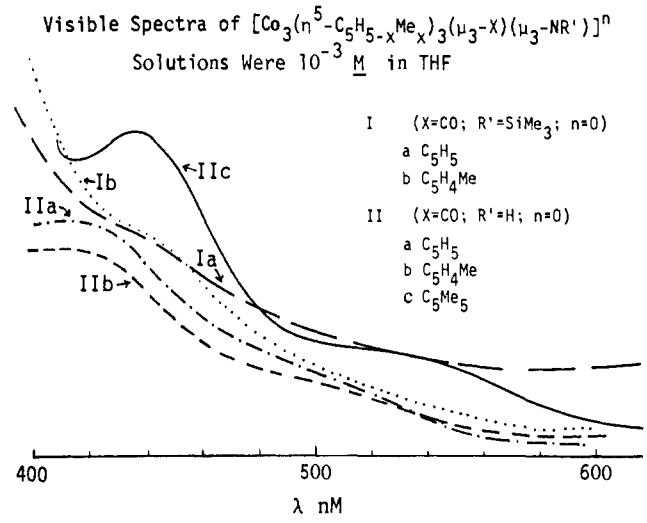

Figure 11. Electronic absorption spectra of the two Me_3SiN-capped clusters (Ia and Ib) and the three HN-capped clusters (IIa, IIb, and IIc) in THF solution (10^{-3} M) in the 400–600-nm region.

On the basis of the approach utilized by Colbran, Robinson, and Simpson[12a] to interpret the electronic absorption spectra of a series of bicapped $Co_3(\eta^5\text{-}C_5H_5)_3(\mu_3\text{-}CH)(\mu_3\text{-}CR)$ clusters, we have assumed that the lowest energy absorption bands correspond to transitions from the HOMO and the next highest filled MO to the LUMO. The lowest energy bands are thereby assigned to an excitation from a "t_{2g}" HOMO. Figure 11 and Table III reveal that each of the three HN-capped clusters has a similar lowest energy band at ca. 500–530 nm; however, this band is conspicuously absent in the visible spectra (Figure 11) for the two Me_3SiN-capped clusters. This spectral difference can be rationalized in terms of the π-acceptor character of the Me_3SiN ligand providing greater energy stabilization of the HOMO relative to its LUMO such that the lowest energy absorption band is blue-shifted to higher energy. Conversely, Figure 11 reveals a red-shift in both spectral bands for the HN-capped clusters on going from the C_5H_5-containing IIa or C_5H_4Me-containing IIb to the C_5Me_5-containing IIc. This spectral shift of both bands in IIc to lower energy is attributed to the greater destabilization of the HOMO relative to the LUMO in IIc due to the more electron-donating C_5Me_5 ligands raising the filled e_1 (ring) orbitals nearer in energy to the 3d Co levels. The resulting HOMO would have greater antibonding C_5Me_5 orbital character due to a greater mixing between the e_1 (ring) and appropriate cobalt orbitals.

Electrochemical Detection of HN Ligand Reactivity in $Co_3(\eta^5\text{-}C_5H_5)_3(\mu_3\text{-}CO)(\mu_3\text{-}NH)$ (IIa). The nitrene ligand in both IIa and IIb did not react with strong bases such as *n*-BuLi and hydrogen atom abstraction reagents such as trityl radical.[13a] However, the following experiment provides convincing evidence for the deprotonation of a triply bridging HN ligand to a "bare" pyramidal-like nitrido-capped ligand from the electrochemically generated dication of IIa. In a typical run, the neutral parent IIa was dissolved in 0.1 M $TBAPF_6/CH_2Cl_2$, and cyclic voltammetric measurements of its reversible 2+/0 reduction couple (for which i_a/i_c = 1) at +0.31 V were recorded (Figure 12A). Upon addition of successive portions of Et_3N by syringe to the electrochemical cell (inside a Vacuum Atmospheres drybox) and subsequent sweeps through the same 2+/0 reduction couple, the peak current (i_c) of the cathodic wave corresponding to the two-electron reduction of the $[IIa]^{2+}$ dication back to the neutral IIa steadily decreased with each added portion of Et_3N whereas the peak current (i_a) of the anodic wave remained unchanged. Upon the addition of a large excess of Et_3N, the cathodic wave essentially disappeared but the anodic oxidation process endured

(31) (a) Olson, W. L. Ph.D. Thesis, University of Wisconsin—Madison, 1984. (b) Olson, W. L.; Stacy, A. M.; Dahl, L. F. *J. Am. Chem. Soc.*, in press.
(32) Chang, D.; Cocolios, P.; Wu, Y. T.; Kadish, K. M. *Inorg. Chem.* **1984**, *23*, 1629–1633.
(33) Hall, M. B.; Fenske, R. F. *Inorg. Chem.* **1972**, *11*, 768–775.
(34) Rives, A. B.; You, X.-Z.; Fenske, R. F. *Inorg. Chem.* **1982**, *21*, 2286–2294.

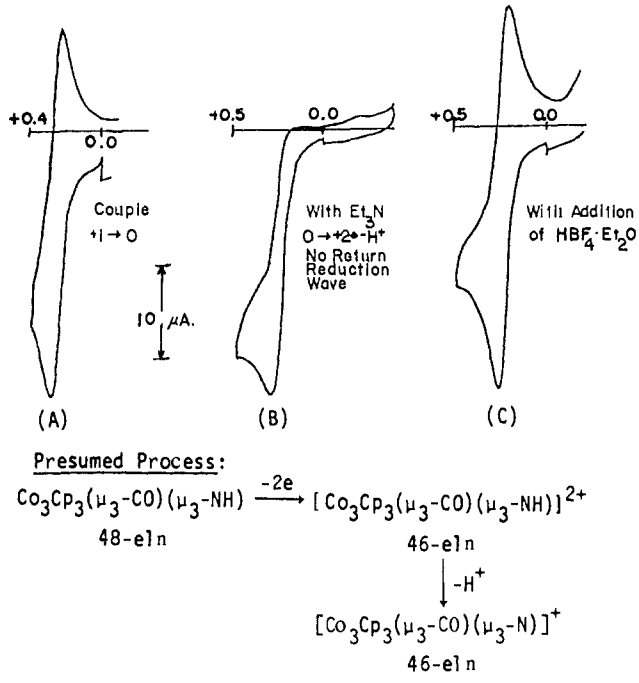

Figure 12. Electrochemical evidence for the deprotonation (with Et_3N) of the electrochemically generated $[Co_3Cp_3(\mu_3\text{-}CO)(\mu_3\text{-}NH)]^{2+}$ dication from $Co_3Cp_3(\mu_3\text{-}CO)(\mu_3\text{-}NH)$ to give a pyramidal nitride cluster. The sequence of CV in measurements on $Co_3Cp_3(\mu_3\text{-}CO)(\mu_3\text{-}NH)$ involves (A) neutral parent in CH_2Cl_2, (B) addition of excess triethylamine to remove acidic protons in solution (A), and (C) addition of excess $HBF_4\cdot Et_2O$ to solution (B).

with its peak current i_a and peak potential E_p being virtually the same as that recorded before Et_3N was added (Figure 12B). The subsequent addition of excess $HBF_4\cdot Et_2O$ by syringe to the bulk solution resulted in a complete return of the anodic wave to give the reversible 2+/0 reduction couple (i_a/i_c = 1) with identical $E_{1/2}$ and E_p values as those before Et_3N was added (Figure 12C).

These experimental results are entirely consistent with a scheme (presented in Figure 12) in which deprotonation by Et_3N of the nitrene (μ_3-NH) ligand in IIa is accomplished only after electrochemical oxidation to a cationic species. As a consequence of the electrochemical removal of two electrons from IIa to form its dication, the relative acidity of the nitrene proton is enhanced to the point where it is easily deprotonated in the presence of an excess of Et_3N. The result of this deprotonation of the $[IIa]^{2+}$ dication is the formation of a pyramidal-like nitrido-capped $[Co_3(\eta^5\text{-}C_5H_5)_3(\mu_3\text{-}CO)(\mu_3\text{-}N)]^+$ monocation which is the conjugate base of $[IIa]^{2+}$. We are currently attempting to isolate and characterize this conjugate-base monocation, an unprecedented example of a pyramidal nitrogen atom coordinated to three transition metals. The synthetic strategy will involve chemical oxidation and subsequent deprotonation of IIa.

Cyclic Voltammetry of the $Ni_3(\eta^5\text{-}C_5H_{5-x}Me_x)_3(\mu_3\text{-}CO)_2$ Series (x = 0, 1): The Fischer–Palm Cluster Reexamined. Representative cyclic voltammograms (at a platinum working electrode) of both the classical Fischer–Palm $Ni_3(\eta^5\text{-}C_5H_5)_3(\mu_3\text{-}CO)_2$ molecule and the methylcyclopentadienyl analogue are presented in Figures 13 and 14, respectively. Both 49-electron clusters show similar electrochemical behavior with one reversible reduction couple and one reversible oxidation couple. The assignment of each of the two couples as a one-electron process is based on the analogous relative peak currents for both couples in each compound together with the reduction couple for the Fischer–Palm molecule having been previously established as a one-electron process from its chemical reduction to the monoanion and resulting crystallographic characterization.[10b]

The electrochemically reversible reduction of the 49-electron Fischer–Palm cluster to its 50-electron monoanion was initially demonstrated in 1966 by Dessy et al.[8] without mention of an oxidation couple for this compound. Unsuccessful attempts in

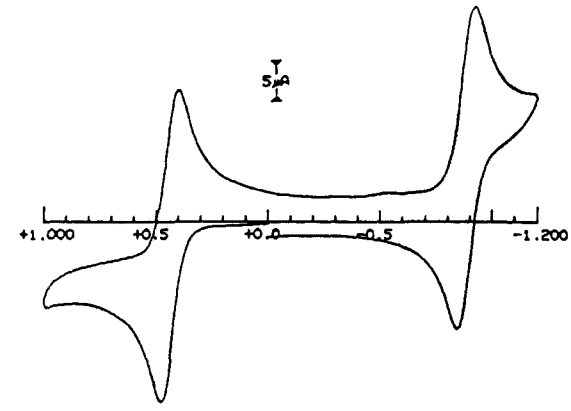

Figure 13. Cyclic voltammogram of the classical Fischer–Palm 49-electron $Ni_3(\eta^5\text{-}C_5H_5)_3(\mu_3\text{-}CO)_2$ in CH_2Cl_2/0.1 M $TBAPF_6$ at a platinum disk electrode with a scan rate of 200 mV/s. A reversible one-electron oxidation, which has not been previously reported, occurs at $E_{1/2}$ = +0.44 V, while the reversible one-electron reduction occurs at $E_{1/2}$ = −0.88 V.

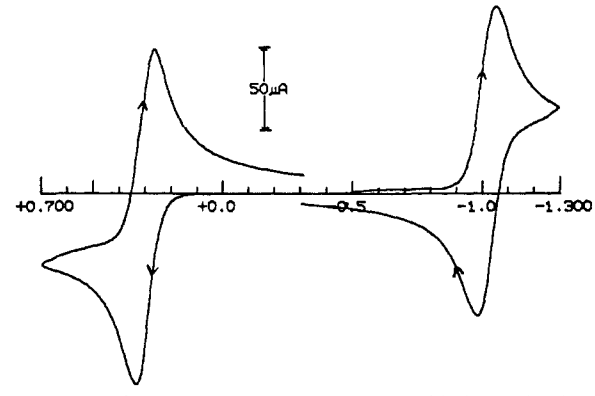

Figure 14. Cyclic voltammogram showing the oxidation and reduction couples of the 49-electron methylcyclopentadienyl $Ni_3(\eta^5\text{-}C_5H_4Me)_3(\mu_3\text{-}CO)_2$ in CH_2Cl_2/0.1 M $TBAPF_6$ at a platinum disk electrode with a scan rate of 200 mV/s. A reversible one-electron oxidation to the 48-electron monocation occurs at $E_{1/2}$ = +0.30 V, and a reversible one-electron reduction to the 50-electron monoanion occurs at $E_{1/2}$ = −1.02 V (vs. SCE). The couples are shown as separate scans to emphasize reversibility.

our laboratories to isolate the 48-electron monocation by chemical oxidation led to the assumption that the 48-electron $Ni_3(\eta^5\text{-}C_5H_5)_3(\mu_3\text{-}CO)_2]^+$ monocation is an unstable species.[10] However, on the basis of the redox behavior (Table II) observed for the 48-electron $[Co_3(\eta^5\text{-}C_5R_5)_3(\mu_3\text{-}X)(\mu_3\text{-}NR)]^n$ clusters (X = CO, n = 0; X = NO; n = 1+) and for the pentamethylcyclopentadienyl $Ni_3(\eta^5\text{-}C_5Me_5)_3(\mu_3\text{-}CO)_2$ analogue,[10b] we concluded that the Fischer–Palm cluster should also undergo reversible oxidation. This hypothesis was substantiated by the detection of a single one-electron reversible oxidation process for both the C_5H_5- and C_5H_4Me-containing nickel clusters.

It is now evident why the early report by Dessy et al.[8] on the redox behavior of $Ni_3(\eta^5\text{-}C_5H_5)_3(\mu_3\text{-}CO)_2$ did not include its reversible one-electron oxidation couple. Their voltammetric measurements of a large variety of organometallic complexes utilized mercury as a working electrode. Subsequent electrochemical investigations[2,12a] have shown mercury to be a relatively poor working electrode for the oxidation of a number of organometallic clusters due to its frequent involvement in adsorption reactions and its proclivity for forming complexes with electrochemically generated cluster ions.[12a]

The redox species electrochemically generated from $Ni_3(\eta^5\text{-}C_5H_5)_3(\mu_3\text{-}CO)_2$ and $Ni_3(\eta^5\text{-}C_5H_4Me)_3(\mu_3\text{-}CO)_2$ are in harmony with those electrochemically accessible from the pentamethylcyclopentadienyl nickel analogue and with those electrochemically produced from the related tricobalt-bicapped clusters (Table II). The $E_{1/2}$ values expectedly show that the methylcyclopentadienyl

nickel analogue is easier to oxidize and harder to reduce than the unsubstiuted Fischer-Palm cluster.

Acknowledgment. This research was made possible by financial support from the National Science Foundation. One of us (R. L.B.) is grateful to the Owens-Corning Fiberglas Corp. (Technical Center: Granville, Ohio) for a Research Fellowship during September 1983-August 1984. We also thank James A. Mahood for preparing a sample of $Ni_3(\eta^5\text{-}C_5H_5)_3(\mu_3\text{-}CO)_2$ for electrochemical measurements.

Registry No. Ia, 53652-62-3; Ib, 103190-57-4; IIa, 103148-47-6; IIb, 103148-48-7; IIc, 103148-49-8; IIIa, 103190-58-5; IIIb, 103190-59-6; IV, 103148-50-1; Va, 103190-60-9; Vb, 103190-61-0; $Ni_3(\eta^5\text{-}C_5H_5)_3(\mu_3\text{-}CO)_2$, 12194-69-3; $Ni_3(\eta^5\text{-}C_5H_4Me)_3(\mu_3\text{-}CO)_2$, 103148-51-2; $Ni_3(\eta^5\text{-}C_5Me_5)_3(\mu_3\text{-}CO)_2$, 103148-52-3; Co, 7440-48-4; Ni, 7440-02-0.

Synthesis and Stereochemical-Electrochemical Investigations of the 49/48-Electron $[Co_3(\eta^5\text{-}C_5H_{5-x}Me_x)_3(\mu_3\text{-}NO)(\mu_3\text{-}NH)]^n$ Series (x = 0, 1; n = 0, 1+): Bonding Analysis of a Marked Redox-Generated Change in Geometry of a Triangular Metal Cluster with π-Acceptor Nitrosyl and π-Donor Nitrene Capping Ligands

Robert L. Bedard and Lawrence F. Dahl*

Contribution from the Department of Chemistry, University of Wisconsin—Madison, Madison, Wisconsin 53706. *Received September 12, 1985*

Abstract: The isolation and structural characterization of the 49-electron $Co_3(\eta^5\text{-}C_5H_4Me)_3(\mu_3\text{-}NO)(\mu_3\text{-}NH)$ (Vb) have been carried out in order to determine the redox-generated variations in geometry of a 49/48-electron trimetal cluster series with mixed π-acceptor and π-donor capping ligands. The preparation and spectral-electrochemical properties of the 49-electron $Co_3(\eta^5\text{-}C_5H_{5-x}Me_x)_3(\mu_3\text{-}NO)(\mu_3\text{-}NH)$ clusters (x = 0; Va; x = 1, Vb) containing π-acidic ON-capping and π-donor (nonhybridized) HN-capping ligands are described. These air-sensitive brownish black compounds were quantitatively obtained by one-electron reductions of their respective $[Co_3(\eta^5\text{-}C_5H_{5-x}Me_x)(\mu_3\text{-}NO)(\mu_3\text{-}NH)]^+$ monocations (x = 0, IIIa; x = 1, IIIb) with cobaltocene in THF. An X-ray diffraction investigation of the methylcyclopentadienyl derivative, Vb, has permitted an unequivocal differentiation between the two possible HOMOs (a_2 and e under C_{3v} symmetry) containing the unpaired electron. The striking structural change in the central $Co_3(NO)(NH)$ core upon the reduction of IIIb to Vb is that the pseudoequilateral cobalt triangle (of average length 2.406 Å) in IIIb undergoes a pronounced deformation in Vb to an isosceles cobalt triangle with *one* much longer Co-Co distance of 2.554 (3) Å and *two* slightly enlarged Co-Co distances of 2.414 (3) and 2.426 (3) Å. This particular distortion of the $Co_3(NO)(NH)$ core from an idealized C_{3v}—$3m$ geometry in IIIb to an idealized C_s—m geometry in Vb is rationalized in terms of a vibronically allowed first-order Jahn-Teller effect which splits the degeneracy of the ^2E ground state under C_{3v} symmetry. The preferential elongation of only one Co-Co bond necessitates that the unpaired electron in Vb occupies a nondegenerate HOMO (a″ under C_s symmetry) which is highly antibonding between the two mirror-related cobalt atoms and thereby *antisymmetric* with respect to the vertical mirror plane. The fact that the Co-C_5H_4Me(centroid) distances for these two mirror-related cobalt atoms are 0.03 Å longer than the third distance in Vb and 0.05 Å longer than the three corresponding distances in IIIb provides persuasive evidence that significant antibonding character between the two cobalt atoms and their attached C_5H_4Me ligands also exists in the HOMO of Vb. Of prime interest is the fact that the observed trimetal distortion in Vb is opposite to the one found in the 49-electron $[Co_3(\eta^5\text{-}C_5H_5)_3(\mu_3\text{-}S)_2]^+$ monoanion (crystallographically characterized both as the iodide and hexafluorophosphate salts) in which the isosceles cobalt triangle has *one* shorter and *two* longer Co-Co bonds. This latter distortion is consistent with the tricobalt antibonding electron being mainly localized between two of the three Co-Co bonds which requires that the half-filled nondegenerate HOMO in the bis(sulfido-capped) cluster is *symmetric* with respect to the vertical mirror plane. To our knowledge, *inverse* Jahn-Teller distortions have not been previously encountered in transition metal cluster chemistry. $Co_3(\eta^5\text{-}C_5H_4Me)_3(\mu_3\text{-}NO)(\mu_3\text{-}NH)$: molecular weight 459.2; triclinic; $P\bar{1}$; a = 9.233 (3) Å, b = 23.750 (7) Å, c = 9.231 (2) Å, α = 96.96 (2)°; β = 119.26 (2)°, γ = 88.28 (3)°, V = 1748.5 (8) Å^3 at -60 °C; D(calcd) = 1.71 g/cm^3 for Z = 4. Anisotropic least-squares refinement converged at $R_1(F)$ = 8.86% and $R_2(F)$ = 10.32% for 3628 independent diffractometry data ($I > 3\sigma(I)$) with a data-to-parameter ratio of 15.1/1. The relatively high discrepancy factors are mainly a consequence of one of the two independent molecules possessing a crystal disorder involving a pseudomirror plane. Hence, the comparative analysis was based upon the "well-behaved" crystal-ordered molecule; the relatively precise structural parameters of its $Co_3(NO)(NH)$ core, which closely conform to C_s—m symmetry, are in accordance with the unambiguous location of the imido hydrogen atom from an electron-density difference map.

Systematic studies of the geometrical effects caused by changes in electronic configuration have been of prime importance in determining the nature of metal-metal bonding in a number of metal cluster systems. The major objective of such studies in our laboratories has been to relate observed structural changes with qualitative metal cluster bonding models possessing energy-level orderings which are dependent on the ligation about the metal cluster core.

Part of our research in this area has focused on the isolation and structural-bonding characterization of paramagnetic monocapped and bicapped triangular metal clusters in order to provide a basic understanding of their electron-transfer properties.

0002-7863/86/1508-5942$01.50/0